EXPLORING THE COMBINED USE OF DISTRIBUTED FIBER AND DEFORMED BAR REINFORCEMENT TO RESIST SHEAR FORCES

Quarterly Progress Report
For the period ending May 31, 2022

Submitted by:
PI: Travis Thonstad
Co-PI: Paolo Calvi
Research Assistant: John Paul Gaston
Research Assistant: Benedikt Farag

Affiliation: Department of Civil and Environmental Engineering
University of Washington

ACCELERATED BRIDGE CONSTRUCTION
UNIVERSITY TRANSPORTATION CENTER

Submitted to:
ABC-UTC
Florida International University
Miami, FL

1. Background and Introduction

Macro-synthetic fibers are often added to concrete mixtures as secondary reinforcement, designed to control shrinkage and temperature cracks and improve the durability of bridge superstructures. The addition of fibers to concrete improves the tensile behavior of the material, which leads to more durable concrete elements with increased ductility and better crack control. In addition to these desirable effects, the tensile strength of the fibers also contributes to the strength of the member, however this benefit is not included in current bridge design specifications [e.g., AASHTO 2020]. The lack of provisions regarding the use of macro-synthetic fibers as supplemental reinforcement is of detriment to the bridge construction industry because the use of fibers in PBEs and cast-in-place connections would result in a reduction of bar reinforcement and congestion, lighter members, smaller crack sizes, better distribution of localized stresses, and increased confinement and performance of member ends.

Developments in PFRCs are applicable to accelerated bridge construction (ABC) in two ways. The use of PFRC would permit thinner prefabricated bridge element (PBE) sections, enabling lighter members for transportation and erection. The great majority of ABC is conducted using PBEs, so any activity that benefits PBEs will encourage the use of them, and by direct implication, ABC. For prestressed girders, the use of PFRC could ameliorate the impacts of thinner girder webs by providing additional web-shear cracking strength, by arresting flexural cracks prior to their development into flexure-shear cracks, and by preventing splitting that would be exacerbated by the reduction in web width, as demonstrated in previous test series of girder end regions [e.g., Haroon et al. 2006]. The improved serviceability and durability of prestressed girders made from FRC would also create an additional incentive for owners to choose ABC techniques over other alternatives. Finally, the use of field-cast PFRC in ABC projects in connection regions would be beneficial by expediting on-site activities, alleviating congestion in connection regions and reducing the required deformed bar reinforcement.

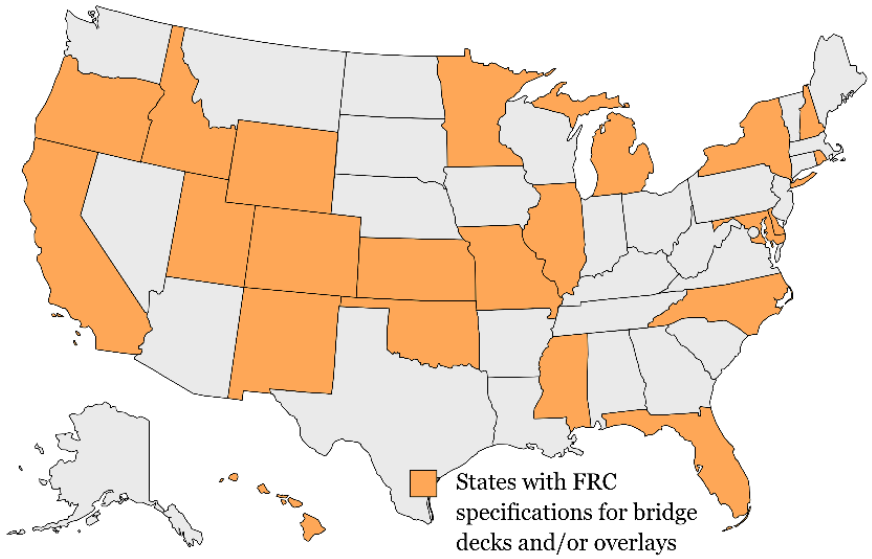

Fig. 1. States with FRC specifications for bridge decks and/or overlays, data from [Amirkhanian and Roesler 2019]

2. Problem Statement

Fiber-reinforced concrete already enjoys widespread use in practice, as shown in Fig. 1, and is required in several states (e.g., California, Oregon, and Delaware) for bridge decks [Amirkhanian and Roesler 2019]. The remaining bridge elements (e.g., prestressed girders) could similarly benefit from the improved strength and durability that FRC provides. To realize the full benefits of PFRC in practice, rational design equations are needed to predict the strength of members containing both macro-synthetic fibers and deformed bar reinforcement, particularly in shear. This research project will result in design guidelines for the combined use of distributed fiber and deformed bar reinforcement to resist shear forces, implementable in future bridge specifications.

3. Objectives and Research Approach

The objective of the proposed research is the development of simple, rational design equations for the contribution of macro-synthetic fibers to the shear strength of reinforced concrete members containing at least the minimum shear reinforcement required by the *AASHTO LRFD Bridge Design Specifications* [AASHTO 2020]. The design equations will be based on a rational shear behavior model that will be developed as part of this work using the response of PFRC panel elements, subjected to in-plane loads (e.g., shear and axial tension or compression). The PI's are uniquely positioned to develop a shear behavior model for PFRC members due to the experimental capabilities available at the University of Washington's (UW) Large-Scale Structural Engineering Testing Laboratory (SETL) and the ability to generate uniform shear stress states using the UW SETL Panel Element Tester. A similar experimental apparatus was used to develop the Modified Compression Field Theory [Vecchio and Collins 1986], which is the basis for the current shear provisions in the *AASHTO LRFD Bridge Design Specifications*. Thus, the experimental data collected will be uniquely suitable for developing the proposed design equations.

4. Description of Research Project Tasks

The following is a description of tasks carried out to date.

Task 1 – Literature Review

This task is complete. The objective of this task is to establish a database to be used to evaluate the design expression developed in Task 3. An extensive review of past experimental research involving polyolefin fiber-reinforced concrete was completed, focusing on specimens that utilized both deformed bar and fiber reinforcement to resist shear forces. The collected data was summarized in the Dec 2022 Progress Report.

Task 2 – Panel testing program

This task is complete. The objective of this task is to elucidate the contributions and benefits of the separate and combined used of deformed bar and macro-synthetic fiber reinforcement. Previous tests of PFRC members did not include deformed bar reinforcement or included only a single deformed bar reinforcement configuration ($\rho_v \approx 0.15\%$ for both test series). This is one of the first experimental programs to specifically investigate the interaction between macro-synthetic fibers (STRUX 90/40) and deformed bar reinforcement in resisting shear forces and provides valuable data that is needed to build a shear behavior model in Task 3.

Fig. 2 shows the normalized shear stress-shear strain behavior for all the panels. To allow comparisons between the tests, the applied shear stress for each panel was normalized by the square root of the average compressive strength of the concrete cylinders tested on the same day as the panel. In general, the panels all had cracking stresses around $2.91\sqrt{f'_c}$ (standard deviation of 0.52 $\sqrt{f'_c}$ with a COV of 18%) and panels with higher transverse reinforcement ratios exhibited greater shear strengths, as anticipated.

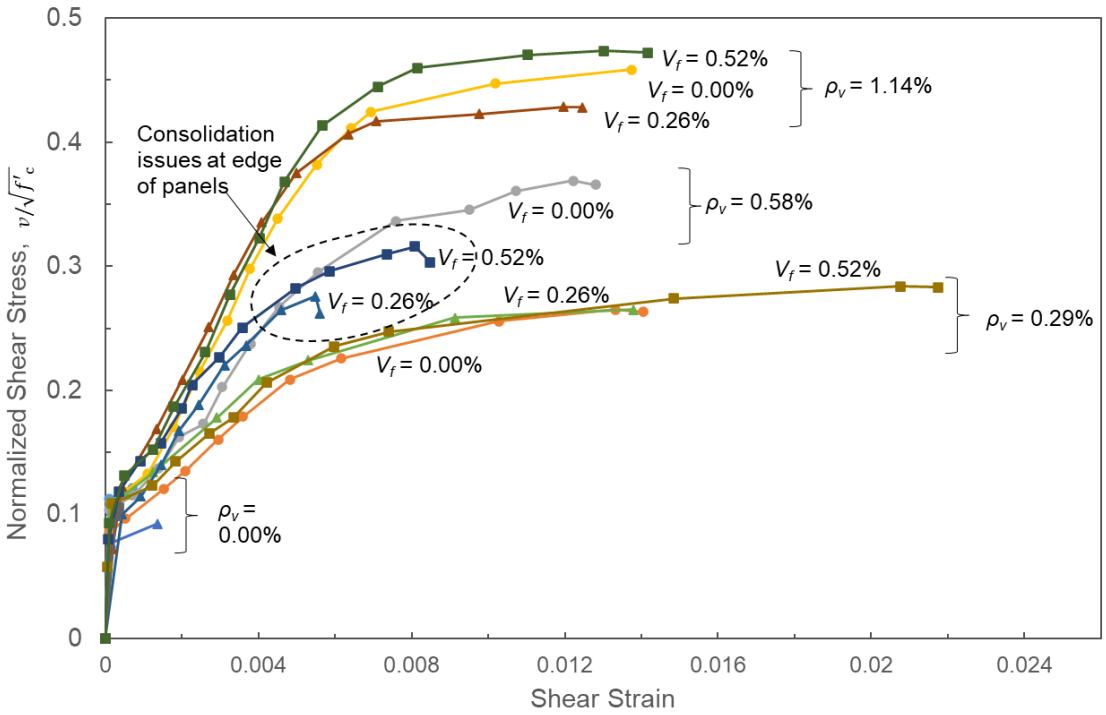

Fig. 2. Normalized shear stress-shear strain behavior for all panels

The principal stresses and strains in the concrete were estimated from the measured data using equilibrium. For an arbitrary i-direction, the relationship between the normal stress in the steel, f_{si}, the normal stress in the concrete, f_{ci}, and the normal applied stress, f_i, was given by Equation 1.

$$f_i = f_{ci} + \rho_{si} f_{si} \tag{1}$$

where ρ_{si} is the reinforcement ratio in the i-direction. Since the tested panels were subjected to pure shear, the applied normal stress in the x- and y-directions were zero, and the stress in the concrete and steel was related using Equation 2.

$$f_{ci} = -\rho_{si} f_{si} \tag{2}$$

To compute the stress in the concrete, the stress in the reinforcement was determined using the elastic modulus of the steel, E_s, and the measured strain in the i -direction, ϵ_i, using Equation 3, which was limited to the measured yield stress of the steel, f_{sy}.

$$f_{si} = \epsilon_i E_s \leq f_{sy} \tag{3}$$

The shear stress in the concrete was assumed to be equal to the applied shear stress, v_{xy}. From these relationships, the principal stresses in the concrete, $f_{c1,2}$, was computed using the stress transformation equation given by Equation 4.

$$f_{c1,2} = \frac{f_{cx}+f_{cy}}{2} \pm \sqrt{\left(\frac{f_{cx}-f_{cy}}{2}\right)^2 + (v_{xy})^2} \quad (4)$$

where the calculated concrete stresses in the x- and y-directions are given by f_{cx} and f_{cy}, respectively, and the applied shear stress is given by v_{xy}. The principal strain orientation, θ_ε, and magnitude, $\varepsilon_{1,2}$, were also be calculated for the panel, in a similar fashion, using Equation 5 and Equation 6.

$$\varepsilon_{1,2} = \frac{\varepsilon_x+\varepsilon_y}{2} \pm \sqrt{\left(\frac{\varepsilon_x-\varepsilon_y}{2}\right)^2 + (\frac{\gamma_{xy}}{2})^2} \quad (5)$$

$$\theta_\varepsilon = \frac{1}{2}\tan^{-1}(\frac{\gamma_{xy}}{\varepsilon_x-\varepsilon_y}) \quad (6)$$

Where ε_x and ε_y are the average strains in the test region in the x- and y-directions, and γ_{xy} is the computed average shear strain in the test region.

Fig. 3 shows the calculated principal tension stress (f_{c1}) and principal compression stress (f_{c2}) for a typical panel specimen (PFRC-026-029) versus the principal tension strain (ε_1) and principal compression strain (ε_2), respectively. The concrete tensile and compression behavior used in the Modified Compression Field Theory (Vecchio and Collins, 1986) are also shown for reference. The principal tension response was initially linear, reached a peak value corresponding to first cracking, and then gradually softened to a value roughly half that of the peak. The panels containing macro-synthetic fibers had higher residual tension strengths when compared to the panels that did not contain fibers. The principal compressive stress-strain response followed a roughly parabolic curve, and the panels failed in shear prior to the principal compressive stress reaching the peak value predicted by the MCFT equations (Vecchio and Collins, 1986). This supports the observation that the panels failed through shear and yielding of the reinforcement rather than by concrete crushing along the compression diagonal.

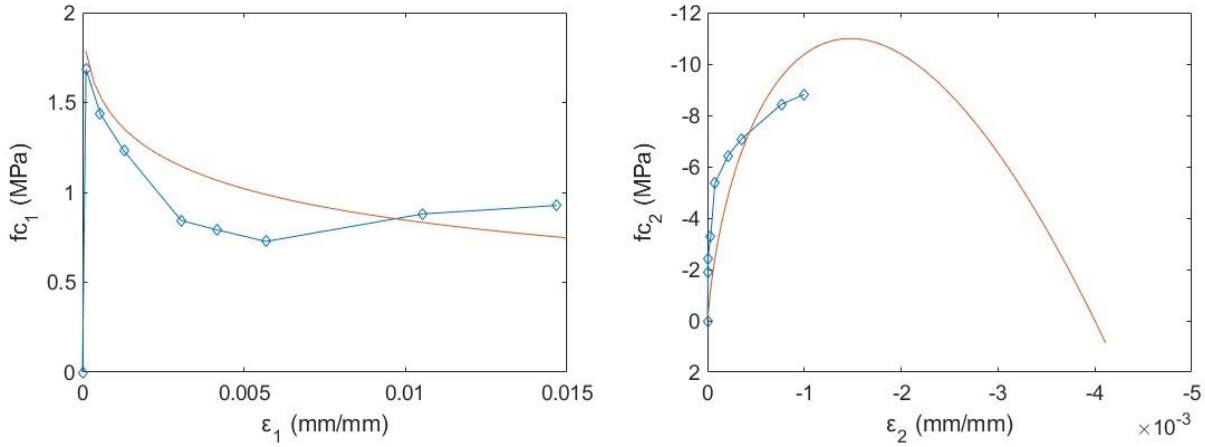

Fig. 3. Principal tensile and compression response of PFRC-026-029

Table 1 summarizes preliminary results from the test series including the cracking stress and strain and values of the shear stress, shear strain, concrete principal stresses, concrete principal strains, crack width, and crack spacing at the final load stage before failure for all twelve panels.

Table 1. Panel Element Test Properties (Note: 1 MPa = 0.145 ksi, 1 mm = 0.0394 in)

Specimen ID	f'_c (MPa)	ν_{cr} (MPa)	γ_{cr} (10^{-3})	ν_u (MPa)	γ_{xy} (10^{-3})	ε_x (10^{-3})	ε_y (10^{-3})	f_{c1} (MPa)	f_{c2} (MPa)	ε_1 (10^{-3})	ε_2 (10^{-3})	f_{sx} (MPa)	f_{sy} (MPa)	w_m (mm)	s_m (mm)
PFRC-000-000	44.5	1.98	0.10	2.12	0.71	0.11	0.42	1.884	-2.388	0.65	-0.13	22.13	87.79	-	-
PFRC-000-029	37.7	1.38	0.11	4.27	13.31	2.04	13.74	1.810	-10.076	16.75	-0.97	428.67	512.43	0.522	109
PFRC-000-058	31.2	1.52	0.10	5.41	12.21	2.76	9.72	2.565	-11.405	13.27	-0.79	512.43	512.43	0.500	69
PFRC-000-114	42.2	1.87	0.16	7.82	13.73	4.21	8.35	5.399	-11.327	13.45	-0.89	512.43	512.43	0.326	64
PFRC-026-000	32.6	1.16	0.15	1.39	1.69	0.81	0.33	0.446	-4.345	1.30	-0.16	171.00	68.63	-	-
PFRC-026-029	38.3	1.80	0.11	4.31	13.80	1.60	11.05	2.215	-8.383	14.68	-2.03	336.66	512.43	0.314	69
PFRC-026-058	34.4	1.54	0.44	4.24	5.49	1.44	4.45	2.720	-6.622	6.08	-0.18	303.43	512.43	0.250	69
PFRC-026-114	43.7	1.25	0.19	7.43	11.95	2.26	7.92	5.382	-10.269	11.71	-1.52	474.32	512.43	0.410	69
PFRC-052-000	29.4	1.41	0.28	1.50	3.59	0.07	0.18	1.340	-1.684	0.31	-0.06	15.08	37.11	-	-
PFRC-052-029	45.0	1.02	0.06	5.00	20.75	2.38	19.75	2.084	-11.988	24.60	-2.46	500.50	512.43	0.470	64
PFRC-052-058	35.5	1.26	0.08	4.94	8.09	2.02	7.04	2.636	-9.275	9.29	-0.23	423.50	512.43	0.297	69
PFRC-052-114	36.1	1.47	0.11	7.47	13.03	2.54	8.52	5.071	-10.999	12.70	-1.63	512.43	512.43	0.426	64

This data is also summarized in the following plots.

Fig. 4 shows the normalized shear strength of all twelve panels plotted against the transverse reinforcement ratio and fiber volume ratio. Also shown is the shear strength of the panels estimated using the AASHTO one-way shear strength equations in Section 5.7.3.4 (AASHTO 2020), assuming an angle of inclination of θ = 45, a strength factor β = 2, a transverse yield stress of f_y=74.3 ksi, and a nominal 28-day concrete compressive strength of f'_c=5.4 ksi. The shear strength of the panels increased with increased to the transverse reinforcement ratio, as expected. The increase in strength was consistent with AASHTO estimates for reinforced concrete elements with transverse reinforcement ratios in the range considered in this study. The normalized shear strength at each reinforcement level, regardless of fiber volume. The main exception was the fiber-reinforced panels at 0.58% transverse reinforcement, which experienced consolidation issues that led to lower strengths.

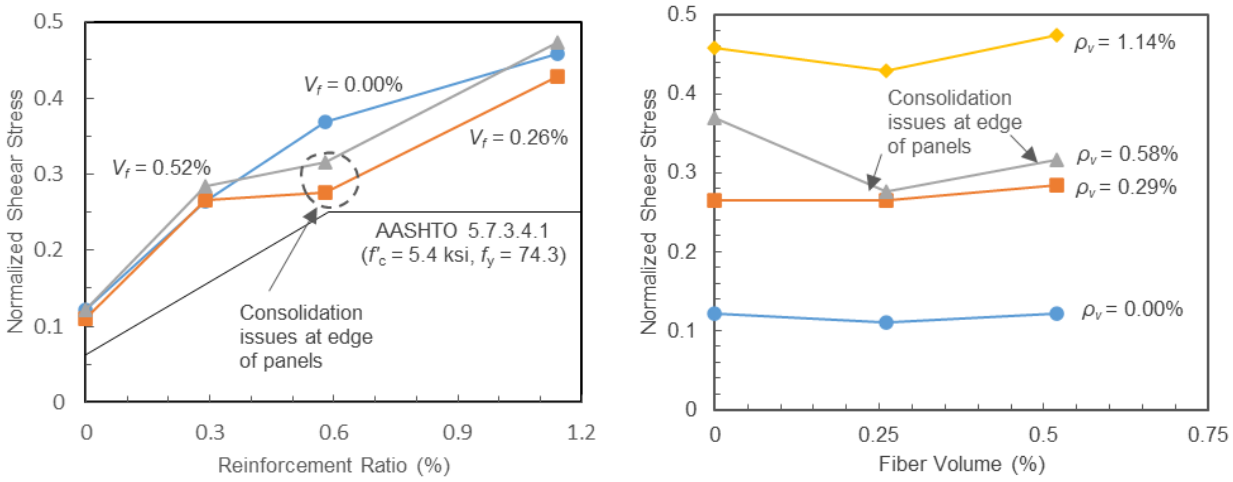

Fig. 4. Normalized shear strength ($\sqrt{f'c}$ in ksi)

Fig. 5 shows the shear strain at failure for all twelve panels plotted against transverse reinforcement ratio and fiber volume ratio. The shear strain at failure increased transitioning from specimens with no shear reinforcement to specimens containing at least the minimum transverse reinforcement required by the AASHTO code (i.e., comparing strain values at 0 and 0.29 transverse reinforcement ratios). The relatively lower maximum shear strain values for the two fiber-reinforced specimens with 0.58% transverse reinforcement, PFRC-026-058 and PFRC-052-058, were attributed to the consolidation issues which occurred in the heavily reinforced edges of those panels that led to premature failure. The influence of fiber volume fraction on the shear strain at failure was found to depend on reinforcement ratio. Panels with 1.14% transverse reinforcement had consistent shear strains at failure despite the addition of fibers. However, at a transverse reinforcement ratio 0% and 0.29%, an increase in shear strain at failure was observed with the addition of macro-synthetic fibers.

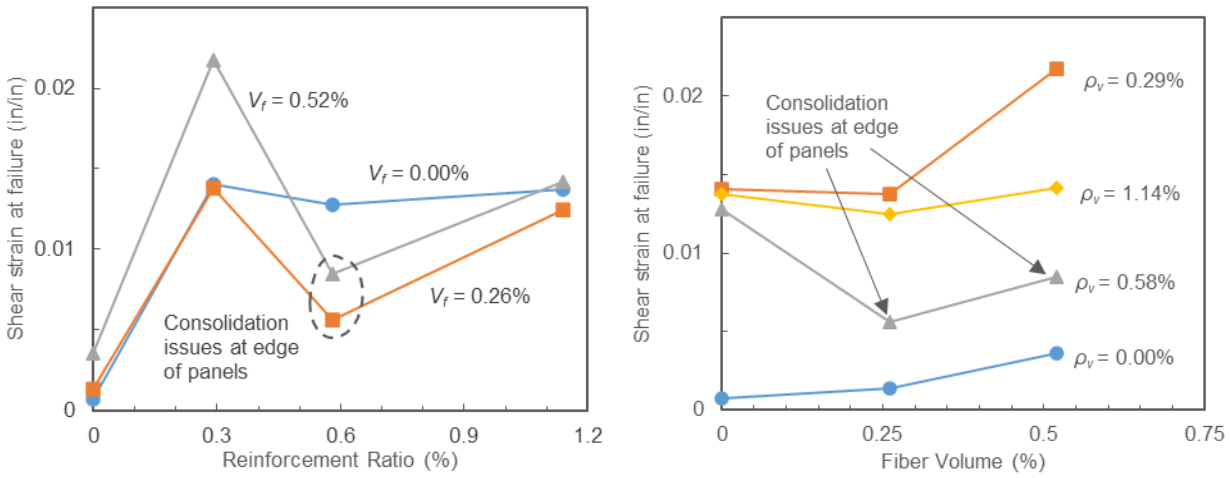

Fig. 5. Shear strain at failure

Fig. 6 shows the average crack width in each panel at a normalized shear stress of $0.13\sqrt{f'c}$ (ksi) versus the reinforcement ratio and fiber volume fraction. The panels without transverse reinforcement did not reach this shear stress level and are, therefore, not shown in the plot. In general, the average crack width at a normalized shear stress of $0.13\sqrt{f'c}$ (ksi) tended to decrease as the transverse reinforcement ratio and fiber volume fraction increased.

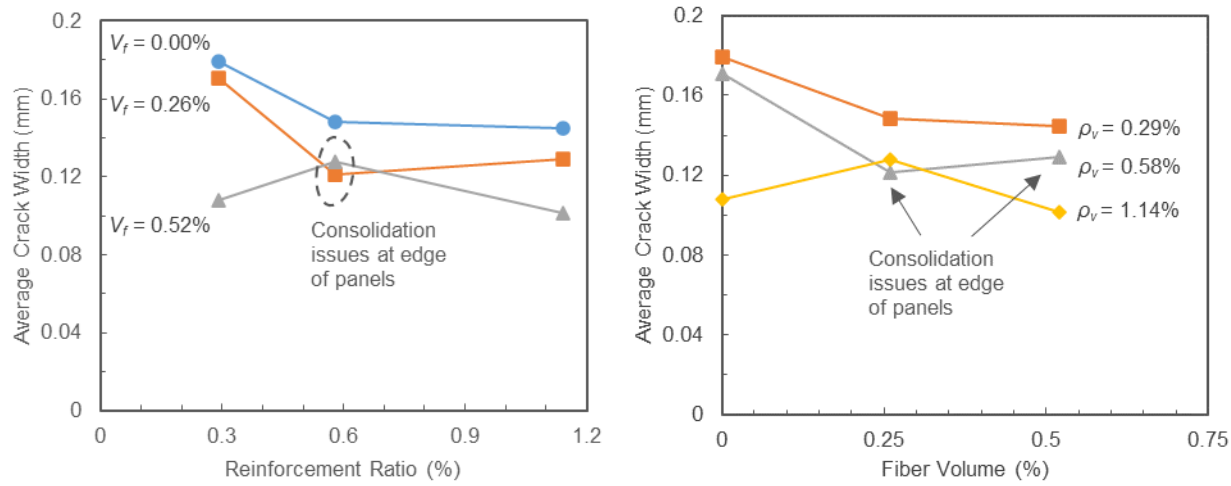

Fig. 6. Average crack width at a normalized shear stress of $0.13\sqrt{f'c}$

Fig. 7 shows the maximum crack width at a normalized shear stress of $0.13\sqrt{f'c}$ (ksi) plotted against transverse reinforcement ratio and fiber volume fraction. The panels without transverse reinforcement did not reach this shear stress level and are, therefore, not shown in the plot. In general, the maximum crack width at a normalized shear stress of $0.13\sqrt{f'c}$ (ksi) tended to decrease as either the transverse reinforcement ratio or fiber volume increased.

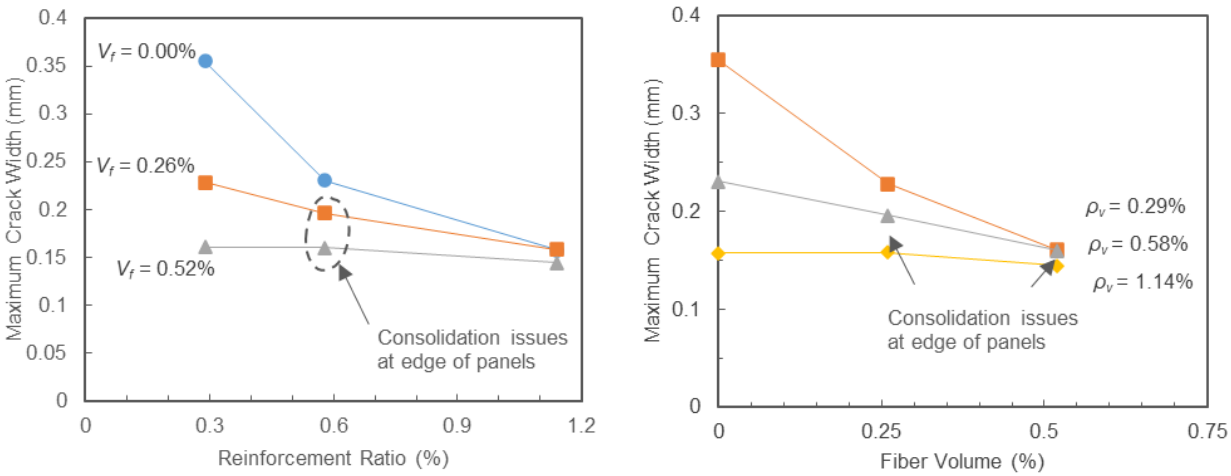

Fig. 7. Maximum crack width at a normalized shear stress of $0.13\sqrt{f'c}$

From the results of the test series, and for the range of the parameters investigated, the following preliminary conclusions were reached:

- Macro-synthetic fibers were effective in decreasing both the maximum and average crack widths during shear loading. For panels with a transverse reinforcement ratio of 0.29%, increasing the fiber volume from 0% to 0.52% reduced the maximum crack width at a shear stress of $0.13\sqrt{f'c}$ (ksi) from 0.35 mm to 0.16 mm (a roughly 50% decrease), and reduced the average crack width from 0.18 mm to 0.14 mm (22% decrease).
- No significant increases in shear strength were observed by adding macro-synthetic fibers at the addition rates used in this study (up to 0.52%). This contrasts with a previous beam test series (Majdzadeh et al. 2006), where the addition of 0.5% macro-synthetic fibers led to a 22% increase in shear strength for beams containing transverse deformed bar reinforcement. These beams had a longitudinal reinforcement ratio of 3.3%, a shear span-to depth ratio of 3.0, and a transverse reinforcement ratio of 0.28%. Other macro-synthetic fiber-reinforced beam tests without stirrups (Altoubat et al. 2009, Greenough & Nehdi 2008) have seen similar increases in shear strength of roughly 20% to 30% with the addition of up to 1% fibers by volume. However, macro-synthetic fiber-reinforced panels without transverse reinforcement have seen no improvement in strength with addition rates of 2% fibers by volume (Carnovale and Vecchio 2014). The discrepancy in results between the beam tests and the panel tests may, therefore, be attributed to the different test methods (pure shear versus concurrent flexure and shear), however further tests are needed to confirm.
- At transverse reinforcement ratios of 0% and 0.29%, the shear strain capacity at failure increased as fiber volume increased, however no improvements to the shear strain capacity were observed at a transverse reinforcement ratio of 1.14%. This is consistent with the results of Carnovale and Vecchio (2014) who found that the addition of fibers to panels containing no transverse reinforcement improved the shear ductility of the panels.
- The benefits of adding macro-synthetic fibers on the shear behavior of structural members may depend on the transverse reinforcement ratio (i.e., there may be more benefit at lower

reinforcement ratios). This is consistent with previous studies (e.g., Altoubat et al. 2009, Greenough & Nehdi 2008) that found a roughly 20% to 30% increase in shear strength for macro-synthetic fiber-reinforced beams without transverse reinforcement.

Task 3 – Development of design recommendations

This task is ongoing. The results of the panel tests in Task 2, will be used to develop design recommendations that capture the potential beneficial interaction between deformed bar and distributed fiber reinforcement. These recommendations will be based on a rational shear behavior model developed for PFRC based on the interactions measured during the experimental testing program (Task 2).

Table 2 shows four empirical equations for the fiber contribution to shear strength proposed in the literature. These relationships were developed for steel fiber-reinforced concrete beams without stirrups (and not for elements that contain both deformed bar and distributed macro-synthetic fiber reinforcement) and were evaluated against the panel test data. The shear strength contribution from the deformed bar reinforcement in the tests was assumed to be $v_s = \rho_v f_{yt}$, where ρ_v is the transverse reinforcement ratio and f_{yt} is the measured yield stress of the transverse deformed bar reinforcement.

Table 2. Empirical equations for predicting the shear strength of fiber-reinforced concrete

Reference	Equation
Swamy & Bahia (1985)	$v_c = 0.517 + 0.283\sigma_{cu}$ (MPa)
Sharma (1986)	$v_c = (2/3)f'_t\left(\frac{d}{a}\right)^2$ (MPa)
Narayanan & Darwish (1987)	$v_c = e\left[0.24f_{spfc} + 80\rho\frac{d}{a}\right] + v_b$ (MPa) $f_{spfc} = \frac{f_{cuf}}{20-\sqrt{F}} + 0.7 + \sqrt{F}$ $F = \left(\frac{L_f}{D_f}\right)V_f d_f$
Kwak, Eberhard, Kim & Kim (2002)	$v_c = 3.7ef_{spfc}{}^{2/3}(\rho\frac{d}{a})^{1/3} + 0.8v_b$ (MPa)

Where:

v_c	is the concrete shear strength;
σ_{cu}	is the flexural strength of fiber-reinforced concrete
a/d	is the shear span-to-depth ratio;
f'_t	is the split-cylinder tensile strength of the concrete;
b_w	is the width of the beam web;
d	is the effective depth of the beam section;
f_{spfc}	is the computed value of the split-cylinder strength of fiber concrete;
ρ	is the flexural reinforcement ratio;
F	is the fiber factor;
e	is an arching factor;

f_{cuf} is the cube strength of fiber concrete in MPa;
L_f is the fiber length;
D_f is the fiber diameter;
V_f is the volume fraction of steel fibers;
d_f is the bond factor;
v_b is the shear strength attributed to fibers, which is taken as $0.41\tau F$;
τ is the bond strength between fibers and concrete matrix; and
e is an arching factor that depends on the span to depth ratio

Fig. 8a shows the predicted panel strength from the empirical equations versus the measured shear strength of the panels. The predicted strengths were computed by summing contributions from the fiber-reinforced concrete and transverse steel reinforcement. The dashed line indicates a 1:1 relationship and the shaded region indicates 20% bounds. Overall, the strengths were overpredicted at lower strength values and were underpredicted at higher strengths with some variation between the empirical equations. The equation developed by Swamy and Bahia (1985) consistently underestimated the strength by nearly 20% and the equation developed by Narayanan and Darwish (1987) tended to give the closest estimates overall for the different strength levels, although the strength of the panels without transverse reinforcement were overestimated by more than 20% (the datapoints with observed strengths less than 2 MPa).

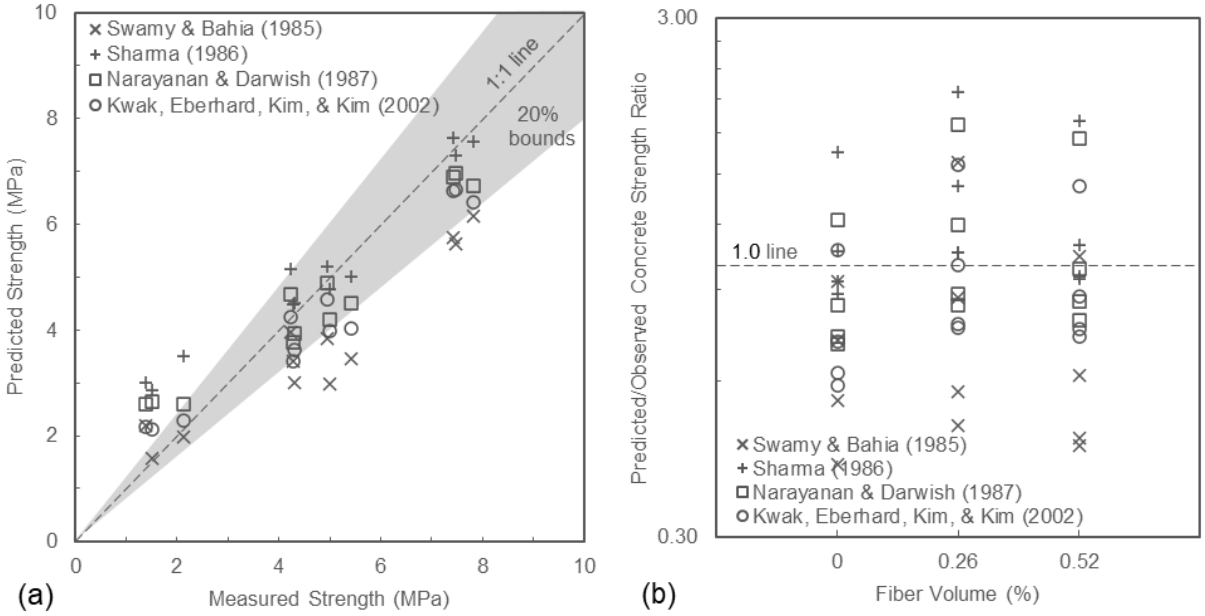

Fig. 8. Comparison with empirical equations (a) Predicted versus measured shear strength of panels (b) ratio of predicted and measured concrete shear strength contributions for panel tests

Fig. 8b shows the ratio of the predicted to the measured concrete strength contribution versus fiber volume ratio. The dashed line indicates a predicted-to-measured concrete strength ratio of 1.0. The measured concrete strengths were computed by subtracting an estimate of the steel contribution to the strength (i.e. $v_s = \rho_v f_{yt}$) from the measured value. This was done so that the denominator in the ratio was roughly the same size, irrespective of reinforcement ratio. Note that the vertical axis is logarithmic to visually show deviation from 1.0 consistently between values that are higher and

lower than the reference line. The equation from Swamy & Bahia (1985) consistently overpredicted the concrete contribution to the strength, the equation from Sharma (1986) consistently underpredicted the concrete contribution to the strength, and the equations from Narayanan & Darwish (1987) and Kwak et al. (2002) were the most consistent with the data with average values of 1.06 and 0.91 and standard deviations of 0.39 and 0.31, respectively.

Task 5 – Interim and Final Reporting

This task in ongoing. The research team will submit timely quarterly reports, present annually at the Research Days meeting, and complete a final report summarizing findings reached during the project.

5. Expected Results and Specific Deliverables

The successful completion of the research project will directly impact the design/construction industry, by providing guidelines for the combined use of distributed fibers and deformed bars to resist shear in field-cast and precast reinforced concrete bridge elements and connections, quantifying the potentially beneficial interaction between the two types of reinforcement.

The expected products resulting from this research will include:

- Database of structural tests of fiber reinforced concrete elements that also contained deformed bars for shear reinforcement,
- Recommended guidelines for the sectional shear strength of PFRC elements with at least the minimum deformed bar shear reinforcement, and
- Design example that demonstrates new design equations.

In addition, the results of the project will be summarized in a 5-min demonstration video and a journal publication.

6. Schedule

Progress on tasks in this project is shown in the tables below.

Item	% Completed
Percentage of Completion of this project to Date	80%

Research Tasks	2022							2023												2024		
	J	J	A	S	O	N	D	J	F	M	A	M	J	J	A	S	O	N	D	J	F	M
Task 1 – Literature Review																						
Task 2 – Panel Testing Program																						
Task 3 – Development of Design Recommendations																						
Task 4 – Interim and Final Reporting																						

7. References

AASHTO (2020) *AASHTO LRFD Bridge Design Specifications (9th Edition)*. American Association of State Highway and Transportation Officials (AASHTO), Washington, DC.

Altoubat, S., Yazdanbakhsh, A., and Rieder, K.A. (2009). Shear behavior of macro-synthetic fiber-reinforced concrete beams without stirrups. *ACI Mat J*, 106(4): 381-389.

Amirkhanian, A. and Roesler, J. (2019) "Overview of Fiber-Reinforced Concrete Bridge Decks." InTrans Report 15-532, Iowa State University, Ames, IA

Carnovale, D. and Vecchio, F.J. (2014). Effect of Fiber Material and Loading History on Shear Behavior of Fiber-Reinforced Concrete. ACI Struct J, 111(5): 1235-1244.

Greenough, T. and Nehdi, M. (2008) "Shear Behavior of Fiber-Reinforced Self-Consolidating Concrete Slender Beams." *ACI Mat J*, 105(5): 468-477.

Kwak, Y.K., Kim, J., Kim, W., & Eberhard, M. (2002). Shear strength of steel fiber-reinforced concrete beams without stirrups. ACI Structural Journal, 99(4).

Majdzadeh, F., Soleimani, S.M., and Banthia. N. (2006). Shear strength of reinforced concrete beams with a fiber concrete matrix. *Canadian J of Civ Eng*, 33: 726–734.

Narayanan, R., & Darwish, I. Y. S. (1987). Use of steel fibers as shear reinforcement. ACI Structural Journal, 84(3).

Swamy, R. N., & Bahia, H. M. (1985). The effectiveness of steel fibers as shear reinforcement. Concrete International.

Sharma, A. K. (1986). Shear strength of steel fiber reinforced concrete beams. ACI Journal Proceedings, 83(4).

Vecchio, F.J. and Collins, M.P. (1986) "The Modified Compression-Field Theory for Reinforced Concrete Elements Subjected to Shear." ACI J, 83 (2): 219–231.